Quantum Accelerator Modes from the Farey Tree

A. Buchleitner,[1] M. B. d'Arcy,[2,*] S. Fishman,[3] S. A. Gardiner,[4,†] I. Guarneri,[5,6,7]
Z.-Y. Ma,[8] L. Rebuzzini,[5,7] and G. S. Summy[9]

[1]*Max-Planck-Institut für Physik komplexer Systeme, D-01187 Dresden, Germany*
[2]*Atomic Physics Division, National Institute of Standards and Technology, Gaithersburg, Maryland 20899-8424, USA*
[3]*Physics Department, Technion, Haifa IL-32000, Israel*
[4]*JILA, University of Colorado and National Institute of Standards and Technology, Boulder, Colorado 80309-0440, USA*
[5]*Dipartimento di Fisica e Matematica, Università degli Studi dell'Insubria, I-22100 Como, Italy*
[6]*Instituto Nazionale per la Fisica della Materia, Unità di Milano, I-20133 Milano, Italy*
[7]*Instituto Nazionale di Fisica Nucleare, Sezione di Pavia, I-27100 Pavia, Italy*
[8]*Department of Physics, University of Oxford, Oxford, OX1 3PU, United Kingdom*
[9]*Department of Physics, Oklahoma State University, Stillwater, Oklahoma 74078-3072, USA*

(Received 21 March 2005; published 24 April 2006)

We show that mode locking finds a purely *quantum* nondissipative counterpart in atom-optical quantum accelerator modes. These modes are formed by exposing cold atoms to periodic kicks in the direction of the gravitational field. They are anchored to generalized Arnol'd tongues, parameter regions where driven nonlinear *classical* systems exhibit mode locking. A hierarchy for the rational numbers known as the Farey tree provides an ordering of the Arnol'd tongues and hence of experimentally observed accelerator modes.

DOI: 10.1103/PhysRevLett.96.164101 PACS numbers: 05.45.Mt, 03.75.Be, 32.80.Lg

Precise control of the state and time evolution of quantum systems is of critical importance in many areas of physics. Tailoring wave packets in Rydberg systems [1], producing single photons on demand [2], creating coherent superpositions of macroscopic persistent-current states [3], and controlling the production of multiparticle entanglement [4], are prominent examples of ''quantum state engineering.'' Although almost perfect control has been achieved over these systems, this can rapidly lose efficiency when influenced by decoherence or noise. Additionally, generic features of strongly coupled quantum systems allow for novel and often robust strategies of quantum control. In such cases, studied in much detail in the area of quantum chaos, peculiar eigenstates emerge which exhibit unexpected localization properties and dynamics, and are remarkably inert with respect to uncontrolled perturbations. Prominent examples are nondispersive wave packets in periodically driven quantum systems [5], quantum resonances [6,7], and stochastic web states [8,9]. These ''strong coupling'' quantum control schemes rely on underlying classical dynamics, which in general is mixed regular chaotic [10]. For such a picture to be meaningful it is in general necessary to approach the semiclassical limit where the classical actions accumulated along typical eigenmodes of the system are large compared to $\hbar$. The quantum system can then ''resolve'' the intricate phase space structure of classically mixed regular-chaotic dynamics, and classical nonlinear stabilization phenomena emerge on microscopic scales.

One of the most ubiquitous of such stabilization phenomena in nonlinear classical dynamics is *mode locking*. Eigenmodes of a periodically driven dissipative system are locked in their time evolution onto the phase of an external drive through a nonlinear resonance phenomenon. It occurs in applications ranging from frequency-stabilized lasers [11] to plasma confinement in fusion reactors [12]. An important question is: is this necessarily strictly a classical/semiclassical effect? We report that features of mode locking occur at the *quantum level* even far from the semiclassical limit. This was achieved using quantum accelerator modes (QAMs) of cold atoms kicked by a pulsed standing wave of light orientated along the Earth's gravitational field [13]. In this Letter we show that the modes observed in these experiments can be classified according to a number-theoretic construction known as the Farey tree [14].

We commence by describing the experimental system which forms the basis of our analysis [13]. To create quantum accelerator modes in the laboratory, laser cooled cesium atoms are exposed to a sequence of equally spaced pulses from a standing wave of light which is far detuned from the nearest atomic transition. Because of the ac Stark effect, the atoms experience each δ-function like pulse as a sinusoidal potential (spatial period $\lambda/2$) proportional to the intensity of the light. A QAM is characterized by a momentum transfer, to a substantial fraction of the atoms, which increases linearly with the number of pulses. Figure 1 shows the momentum of the atomic ensemble as a function of pulse period T with the accelerator modes highlighted by the labeled curves [13]. The inset plots the momentum distribution of a $(1, 0)$ QAM as a function of the number of pulses. Note how the width and amplitude of the accelerator mode (the peak which moves to the left) remain relatively unchanged and the center momentum increases linearly with pulse number. This can be contrasted with the peak near zero momentum which broadens

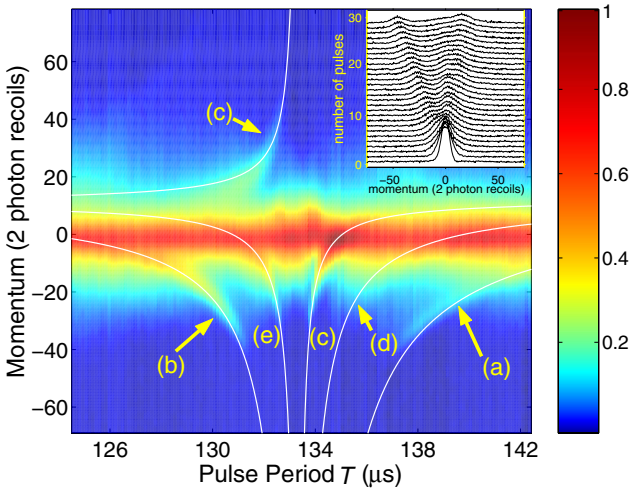

FIG. 1 (color online). Density plot of experimental atomic momentum distributions (measured in a frame falling freely with g) after $n = 30$ pulses as T is varied in the vicinity of $T_2 = 133.3\ \mu$s, from 124.5 μs to 142.5 μs in steps of 0.128 μs [13]. The labels (a), (b), and (c) indicate (2, 1), (3, 1), and (5, 2) quantum accelerator modes, as predicted by the corresponding Arnol'd tongues depicted in Fig. 3. Labels (d) and (e) indicate (7, 3) and (8, 3) modes. White lines are the momenta predicted by Eq. (3). Inset shows the evolution of a typical [in this case a (1, 0)] QAM as a function of pulse number. The color bar indicates the population scale.

as pulses are applied. Although the stability of the accelerator mode from pulse-to-pulse is already somewhat reminiscent of mode locking behavior, there are other reasons to think of the accelerator mode in this way.

To see this, we examine the atomic center-of-mass dynamics using the one-dimensional δ-kicked accelerator Hamiltonian $\hat{H} = \hat{p}^2/2m + mg\hat{z} - \hbar\phi_d[1 + \cos(G\hat{z})] \times \sum_n \delta(t - nT)$ [15]. Here $\hat{z}$ is the vertical position, $\hat{p}$ the momentum, m the atomic mass, g the gravitational acceleration, t the time, $G = 4\pi/\lambda$ [16], and $\phi_d = U_0 t_p/2\hbar$, where U_0 is the maximum ac Stark shift in the standing wave and t_p is the pulse duration. The special resonant values of T in the vicinity of which QAMs occur experimentally are $T_l = 2\pi lm/(\hbar G^2) = l \times 66.7\ \mu$s, with l any non-negative integer. Hence, $\epsilon = 2\pi l(T/T_l - 1)$ is a small parameter. Translating to a frame accelerating with g, to remove the linear potential, and taking the limit $\epsilon \to 0$ the quantum dynamics of the kicked atoms can be modeled by the classical map [17]:

$$J_{n+1} = J_n - K\sin(\theta_n) - \mathrm{sgn}(\epsilon)2\pi\Omega, \tag{1a}$$

$$\theta_{n+1} = \theta_n + \mathrm{sgn}(\epsilon)J_{n+1} \bmod (2\pi), \tag{1b}$$

where $\mathrm{sgn}(\epsilon)$ is positive (negative) if the pulse interval T is greater (smaller) than T_l, and

$$\theta = Gz \bmod (2\pi), \tag{2a}$$

$$J_n = I_n + \mathrm{sgn}(\epsilon)[\pi l + \beta\tau - 2\pi\Omega(n + 1/2)], \tag{2b}$$

with $p/\hbar G = I/|\epsilon| + \beta$, $K = \phi_d|\epsilon|$, $\Omega = gGT^2/2\pi$, and $\tau = 2\pi lT/T_l$. Note that the deeply quantum mechanical character of the atomic dynamics remains hidden in the parametrization of Eqs. (1) and (2) through the quasimomentum β, $0 \le \beta < 1$, since the limit $\epsilon \to 0$ leading to the classical Eqs. (1) leaves the finite value of $\hbar$ unaffected. By Bloch theory, subspaces of different quasimomenta are decoupled.

Mode locking enters the theory of QAMs via Eq. (1) which also describes the deterministic motion of a periodically kicked classical particle on a circle. In this case θ_n and J_n are the angle and angular momentum just before the nth kick, K is the kicking strength, and Ω the unperturbed winding number. If the classical particle is additionally subject to dissipative forces, the accessible phase space shrinks, and Eq. (1) reduces (in the long-time limit) to the sine-circle map [18]: $\theta_{n+1} = \theta_n - K\sin(\theta_n) - 2\pi\Omega$, a paradigm in the study of mode locking. If $K = 0$ and Ω is a rational number $\mathfrak{m}/\mathfrak{p}$, any trajectory of the sine-circle map returns to its initial value (modulo 2π) after $\mathfrak{p}$ iterations. For $0 < K < 1$, mode locking is observed; over a range of Ω values around $\mathfrak{m}/\mathfrak{p}$ (the mode locking interval) a periodic trajectory with rational winding number $\mathfrak{m}/\mathfrak{p}$ *persists*. This orbit attracts all other orbits asymptotically in time, such that finally all have this winding number. The widths of the mode locking intervals are exponentially small in $\mathfrak{p}$, and increase with increasing K up until $K = 1$. The regions thus formed in (Ω, K) parameter space, terminating at $K = 0$, $\Omega = \mathfrak{m}/\mathfrak{p}$, are known as *Arnol'd tongues* [19].

Using this formalism, it is now possible to analyze the dynamics of the QAM in the $\epsilon \to 0$ limit. To begin we look for stable periodic orbits in Eq. (1) such that, if (J_0, θ_0) is on an order $\mathfrak{p}$ orbit, after $\mathfrak{p}$ pulses $J_\mathfrak{p} \bmod (2\pi) = J_0$. If the orbit is stable, then each of the $\mathfrak{p}$ points it is composed of is surrounded by a nonlinear resonance island, set in a chaotic sea, where the motion is predominantly regular; the motion in the island system approximates that of the periodic orbit. If the orbit has winding number $\mathfrak{m}/\mathfrak{p}$, then $J_\mathfrak{p} = J_0 + 2\pi\mathfrak{m}$. Thus, from Eq. (2), I_n (and therefore p_n) grows linearly with time. The islands travel in momentum, resulting in acceleration. If a wave packet is launched within an island surrounding a stable periodic orbit, the acceleration of the corresponding QAM obeys

$$p_n \simeq p_0 + n\frac{2\pi}{|\epsilon|}\left(\Omega - \frac{\mathfrak{m}}{\mathfrak{p}}\right)\hbar G, \tag{3}$$

precisely as observed in the inset of Fig. 1. Hence, we can identify QAMs with nonlinear resonance islands in the classical phase space generated by Eq. (1). This is just another manifestation of the general mode locking phenomenon we are describing here. These islands are robust structures, as guaranteed by the Kolmogorov-Arnol'd-Moser (KAM) theorem [20]. A quantum wave packet initially prepared in the island travels with it, and decays only slowly by tunneling into the chaotic surroundings. For sufficiently small ϵ, this tunneling is exponentially weak,

resulting in a stable QAM. More importantly, due to the KAM theorem the island itself is rather inert with respect to perturbations of the Hamiltonian generating the map Eq. (1). This robustness is inherited by the QAMs and shields them against experimental noise [5].

In Fig. 2 we plot a "phase diagram" to represent the regions (tongues) where stable periodic orbits with different values of $(\mathfrak{p}, \mathfrak{m})$ are numerically observed in the (Ω, K) parameter plane. This plot contains the parameter space explored experimentally [13] using values of T in the vicinity of $T_2 = 133.3\ \mu$s. Close to $K = 0$, each of the stable periodic orbit regions is wedge-shaped, with its vertex at $\Omega = \mathfrak{m}/\mathfrak{p}$, $K = 0$. Moving to higher K inside a tongue, the periodic orbit eventually turns unstable. A sequence of bifurcations follows, which breaks the tongue into fragments. Fragments of different tongues intertwine and overlap in complicated ways. A tongue may be overlapped by others even before breaking, and such overlaps persist even at quite small values of K.

Using a canonical perturbation theory [20–22] to determine an existence condition for a stable periodic orbit for Eq. (1) with a given $(\mathfrak{p}, \mathfrak{m})$, one obtains, $|K| > 2\pi\sqrt{\mathfrak{p}}|\Omega - \mathfrak{m}/\mathfrak{p}|$. In the form of an equality, this equation accurately bounds the wedge-shaped $(\mathfrak{p}, \mathfrak{m})$ tongue near its vertex. This is shown for the (21, 8) and (5, 2) periodic orbits by dashed lines in Fig. 2. Numerical computation and scaling considerations reveal the "critical region" where a tongue breaks to be roughly located at kicking strengths $K \sim 2\pi\mathfrak{p}^{-3/2}$ [22]. Thus, the higher the period of an orbit, the narrower the corresponding tongue, and the lower the "critical value" of K at which the tongue begins to break.

The parameters corresponding to a specific experiment determine a point in the phase diagram. If this point is inside a tongue then a QAM may be observed. At fixed pulse number n, Eq. (3) defines a curve of enhanced population in the (T, p) plot (seen in the data of [13] presented in Fig. 1), due to the presence of the $(\mathfrak{p}, \mathfrak{m})$ QAM. We explore the phase diagram of Fig. 2, keeping both ϕ_d and n constant, while varying T. This procedure varies ϵ, K and Ω. The results of such an experiment are shown in Fig. 1. The locus of the experimentally explored points in the phase diagram is a curve shown by the dotted line in Figs. 2 and 3. This curve hits the $K = 0$ axis at $\Omega' = gGT_l^2/2\pi$, the value of Ω corresponding to the exactly-resonant value of the kicking period $T = T_l$. This is 0.3902 when $l = 2$.

Perhaps most remarkably, the values of $\mathfrak{m}$ and $\mathfrak{p}$ corresponding to experimentally observable QAM are determined by the Farey hierarchy of rational numbers [14]. This representation of rational numbers is a generic feature of mode locking phenomena normally observed in systems

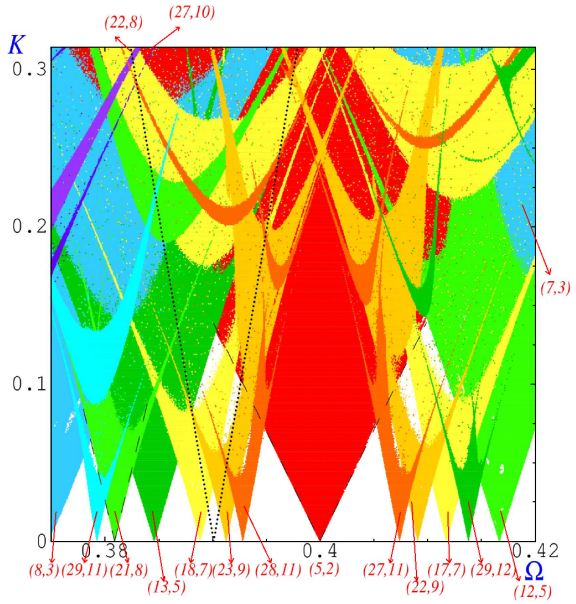

FIG. 2 (color online). Arnol'd tongues' structure. Different colors identify different tongues associated with different quantum accelerator modes. The dotted line marks the locus of experimentally explored points when $T \sim T_2$; dashed lines bound regions for which (21, 8) and (5, 2) stable periodic orbits exist, as specified by $|K| > 2\pi\sqrt{\mathfrak{p}}|\Omega - \mathfrak{m}/\mathfrak{p}|$.

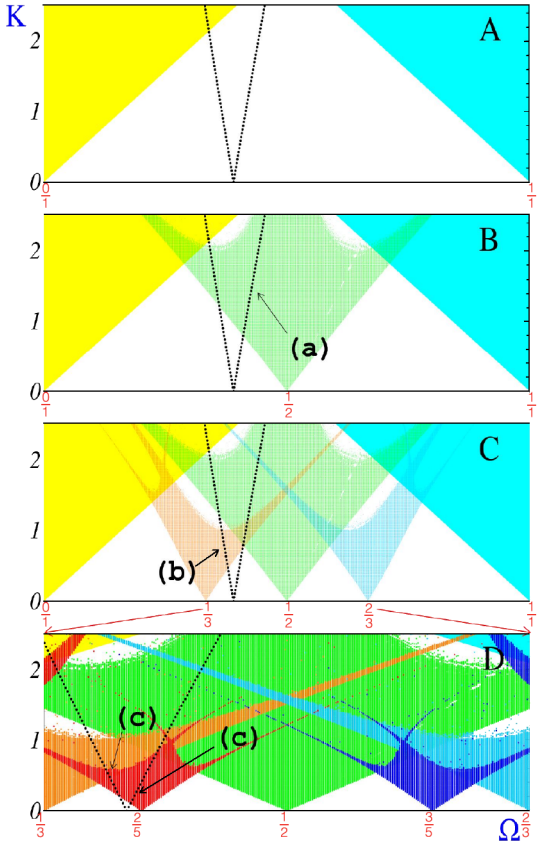

FIG. 3 (color online). Operation of the Farey recursion, moving from frames A to D, for determining the experimentally observed (2, 1), (3, 1), and (5, 2) quantum accelerator modes. The dotted line indicates the locus of the experimentally explored points, while the labels (a), (b), and (c) mark the regions in which accelerator modes are observed. The labels correspond to those used in Fig. 1.

with dissipation. In this hierarchy all rational numbers in $[0, 1]$ are constructed as follows: Start from the pair $(\frac{0}{1}, \frac{1}{1})$. At the second level the fraction $\frac{1}{2} = \frac{0+1}{1+1}$ is introduced so that the series consists of $(\frac{0}{1}, \frac{1}{2}, \frac{1}{1})$. On the next level the fractions $\frac{1}{3} = \frac{0+1}{1+2}$ and $\frac{2}{3} = \frac{1+1}{2+1}$ are added. This process is continued so that if $r_1 = \frac{\mathfrak{m}_1}{\mathfrak{p}_1}$ and $r_2 = \frac{\mathfrak{m}_2}{\mathfrak{p}_2}$ are adjacent irreducible fractions at some level, the first rational to be added between them at the next level is their Farey mediant $r = \frac{\mathfrak{m}_1+\mathfrak{m}_2}{\mathfrak{p}_1+\mathfrak{p}_2}$. At no level can a rational with a denominator smaller than $\mathfrak{p}_1 + \mathfrak{p}_2$ be found between r_1 and r_2. At each level the interval $[0, 1]$ is thus divided by the Farey fractions into Farey subintervals. As the experimental line approaches Ω' in Fig. 3, it successively intersects tongues specified by values of $(\mathfrak{p}, \mathfrak{m})$; these values determine the observed QAM. The ratios $\mathfrak{m}/\mathfrak{p}$ are increasingly close approximations to Ω'.

To determine the tongues (and hence QAMs) appearing in the experiment, we start from orbits with small $\mathfrak{p}$. In Fig. 3(a) the $(1, 0)$ and $(1, 1)$ tongues are presented (their vertices, at $K = 0$, are outside the boundaries of Fig. 2). These correspond to the first numbers in the Farey hierarchy. The dotted line marking the experimental points intersects (within the boundaries of the figure) the $(1, 0)$ tongue. In the region of intersection the stable orbit $(1, 0)$ is found. The corresponding QAMs exhibit rapid acceleration, and at $n = 30$ pulses they move beyond the experimental window shown in Fig. 1. For higher-order QAMs, higher orders of the Farey hierarchy are required. At the second level the $(2, 1)$ tongue, shown in Fig. 3(b), is introduced, and Ω' is in the interval $[\frac{0}{1}, \frac{1}{2}]$. The experimental line intersects the $(2, 1)$ tongue, so a $(2, 1)$ orbit (and QAM) is found. Corresponding points are marked by (a) in Figs. 1 and 3(b). The third level [Fig. 3(c)] introduces the $(3, 1)$ and $(3, 2)$ tongues. The experimental line intersects both these tongues, yet only the $(3, 1)$ QAM is observed [intersection region marked by (b) in Figs. 1 and 3(c)]. This is because $\frac{2}{3}$ is further than $\frac{1}{3}$ from Ω', and so the intersection with the $(3, 2)$ tongue takes place in a region where $K > 2\pi\mathfrak{p}^{-3/2}$. There are only narrow remnants of the tongue, and the corresponding stable island is too small for a QAM to be observable. The relevant Farey subinterval is now $\frac{1}{3}$ to $\frac{1}{2}$. The construction can be continued in similar fashion. In Fig. 3(d) the $(5, 2)$ and $(5, 3)$ tongues are introduced. Since both lines have a large overlap with the $(5, 2)$ tongue [regions marked with (c)], the corresponding QAM appears on both sides of the resonance. Proceeding would ideally produce all the Farey subintervals in which Ω' belongs. Faint traces of QAMs that lie outside this recursion may also be detected, e.g., the white curve (d) in Fig. 1 corresponds to a $(7, 3)$ mode. Note how in the experimental data it is disfavored in comparison with the $(8, 3)$ mode [curve (e)], as $\frac{3}{8}$ is closer than $\frac{3}{7}$ to Ω'.

This construction demonstrates how the Farey tree classifies the complex structure of overlapping tongues according to those that are most important for the description of QAMs observed for a specific value of Ω'. Furthermore, as $K \to 0$, the value of $\frac{\mathfrak{m}}{\mathfrak{p}}$ for the QAMs seen in the experiment converges to Ω'. As Ω' is determined by the local value of gravity, we obtain systematically improving rational approximants of g. The underlying *classical* mode locking mechanism thus renders *quantum* accelerator modes a robust tool for efficient quantum state control, deep in the quantum realm.

We acknowledge support from the Royal Society, the Lindemann Trust, the US-Israel BSF, the Minerva Centre of Nonlinear Physics of Complex Systems, NASA, the Clarendon Bursary, the UK EPSRC, the Israel Science Foundation, and the EU TMR "Cold Quantum Gases" Network.

*Present address: Department of War Studies, King's College London, London WC2R 2LS, United Kingdom.
†Present address: Department of Physics, Durham University, Durham DH1 3LE, United Kingdom.

[1] T. Weinacht, J. Ahn, and P. Bucksbaum, Phys. Rev. Lett. **80**, 5508 (1998).
[2] S. Brattke, B. Varcoe, and H. Walther, Phys. Rev. Lett. **86**, 3534 (2001).
[3] C. van der Wal *et al.*, Science **290**, 773 (2000).
[4] C. Roos *et al.*, Science **304**, 1478 (2004).
[5] H. Maeda and T. F. Gallagher, Phys. Rev. Lett. **92**, 133004 (2004).
[6] W. H. Oskay *et al.*, Opt. Commun. **179**, 137 (2000).
[7] M. B. d'Arcy *et al.*, Phys. Rev. Lett. **87**, 074102 (2001).
[8] T. M. Fromhold *et al.*, Nature (London) **428**, 726 (2004).
[9] A. R. R. Carvalho and A. Buchleitner, Phys. Rev. Lett. **93**, 204101 (2004).
[10] A. Buchleitner, D. Delande, and J. Zakrzewski, Phys. Rep. **368**, 409 (2002).
[11] M. Sargent, M. O. Scully, and W. E. Lamb, *Laser Physics* (Addison Wesley, Reading, MA, 1974).
[12] J. B. Taylor and B. V. Chirikov, Phys. Rev. Lett. **33**, 1139 (1974).
[13] S. Schlunk *et al.*, Phys. Rev. Lett. **90**, 124102 (2003).
[14] J. Farey, Philos. Mag. **47**, 385 (1816); G. H. Hardy and E. M. Wright, *An Introduction to the Theory of Numbers* (Clarendon, Oxford, 1979).
[15] M. B. d'Arcy *et al.*, Phys. Rev. E **64**, 056233 (2001).
[16] $\hbar G$ is therefore equal to two photon recoils.
[17] S. Fishman, I. Guarneri, and L. Rebuzzini, Phys. Rev. Lett. **89**, 084101 (2002); J. Stat. Phys. **110**, 911 (2003); R. Bach *et al.*, Phys. Rev. A **71**, 033417 (2005).
[18] H. G. Schuster, *Deterministic Chaos, an Introduction* (VCH, Weinheim, 1995).
[19] M. H. Jensen, P. Bak, and T. Bohr, Phys. Rev. A **30**, 1960 (1984).
[20] A. J. Lichtenberg and M. A. Lieberman, *Regular and Chaotic Dynamics* (Springer-Verlag, New York, 1992).
[21] B. V. Chirikov, Phys. Rep. **52**, 263 (1979).
[22] I. Guarneri, L. Rebuzzini, and S. Fishman, Nonlinearity **19**, 1141 (2006).